J. Membrane Biol. 41, 265–293 (1978)

Ion Transport across the Isolated Intestinal Mucosa of the Winter Flounder, *Pseudopleuronectes Americanus*

I. Functional and Structural Properties of Cellular and Paracellular Pathways for Na and Cl

Michael Field*, Karl J. Karnaky, Jr.**, Philip L. Smith, Jennifer E. Bolton, and William B. Kinter

Mt. Desert Island Biological Laboratory, Salsbury Cove, Maine 04672, and the Departments of Medicine, Thorndike Laboratory and Gastrointestinal Unit of Beth Israel Hospital and Harvard Medical School, Boston, Massachusetts 02215

Received 13 February 1978

Summary. The isolated intestinal mucosa of the flounder, *Pseudopleuronectes americanus*, when bathed in a 20 mM HCO_3-Ringer's solution bubbled with 1% CO_2 in O_2, generated a serosa-negative PD and, when short-circuited, absorbed Cl at almost 3 times the rate of Na. Reducing HCO_3 to 5 mM decreased the net Cl flux by more than 60%. The following results suggest that, despite the PD, Na and Cl transport processes are nonelectrically coupled: replacing all Na with choline abolished both the PD and net Cl flux; replacing all Cl with SO_4 and mannitol abolished the PD and the net Na flux; and adding ouabain (to 0.5 mM) abolished the PD and the net Cl flux. Nearly all of the unidirectional serosa-to-mucosa Cl flux (J_{sm}^{Cl}) seemed to be paracellular since it varied with PD and Cl concentration in a manner consistent with simple diffusion. J_{sm}^{Cl} was only about one-fourth of J_{sm}^{Na}, suggesting that the paracellular pathway is highly cation-selective. The data can be explained by the following model: (i) Na and Cl uptake across the brush border are coupled 1:1; Na is pumped into the lateral space and Cl follows passively, elevating the salt concentration there; (ii) the tight junction is permeable to Na but relatively impermeable to Cl; and (iii) resistance to Na diffusion is greater in the lateral space (considered in its entirety) than in the tight junction. If these assumptions are correct, the serosa-negative transmural PD is due mainly to a salt diffusion potential across the tight junction and, under short-circuit condition, most of the Na pumped into the lateral space diffuses back into the luminal solution, whereas most of the Cl enters the serosal solution. Morphological features of the epithelium support this interpretation: the cells are unusually long (60 μm) and narrow (3.5 μm); there is little distension of the apical 12 μm of the lateral space during active fluid absorption; and distension distal to this region is intermittently constricted by desmosomes.

* *Present address and to whom request for reprints should be addressed:* Department of Medicine, Box 400, University of Chicago, 950 E. 59th Street, Chicago, Illinois 60637.
** *Present address:* Department of Anatomy, Temple University School of Medicine, Philadelphia, Pa. 19140.

0022-2631/78/0041-0265 $05.80

The intestines of certain marine teleosts, when bathed on both sides with identical Ringer's solutions, generate a serosa-negative PD [1, 2, 21, 23, 43] and, when also short-circuited, absorb Cl faster than Na [2]. This behavior contrasts to that of amphibian [36], reptilian [17] and mammalian [12, 33, 42] small intestine which exhibit a serosa-positive transmural PD and, when short-circuited, absorb Na at a rate at least equal to that of Cl.

Because of these differences, we have examined the relation between Na and Cl transport processes in flounder intestinal epithelium. Our data indicate that net fluxes of Na and Cl are nonelectrically coupled and suggest that the Cl predominance arises from the permselective and resistive properties of the paracellular shunt pathway. In order to further explore these relationships, we have also examined the structure of flounder intestinal mucosa during active fluid absorption using light and electron microscopic techniques.

Materials and Methods

Physiological Studies

Flounder were caught in nets off of Mount Desert Island, Maine, and maintained at 14–16 °C in a large tank of running sea water for at least 48 hr prior to use. Fish weighing from 200 to 600 g were killed by a blow to the head and the intestine was quickly removed, opened longitudinally and rinsed with cold, buffered saline. Beginning about 4 cm below the stomach, four 2 cm segments were stripped of muscle (both layers) and mounted in Ussing chambers as previously described for rabbit ileum [12]. Two sizes of chambers were employed: initially a chamber which exposed 1.12 cm^2 of mucosa and subsequently a smaller one which exposed 0.64 cm^2. Several Ringer's solutions (10 ml per reservoir) were employed: (i) A high HCO_3, NaCl solution containing in mmol/liter: Na, 168; K, 5; Ca, 1; Mg, 1; Cl, 150; HCO_3, 20; HPO_4, 2; and SO_4, 2; (ii) a low HCO_3, NaCl solution: Na, 157; Cl, 157; HCO_3, 5; no SO_4 and the remaining ions as above; (iii) a Na-free Ringer's which was the same as High HCO_3-Ringer's except that choline replaced all Na; and (iv) a Cl-free Ringer's which contained 75 mM SO_4 and 75 mM mannitol to replace all Cl but was otherwise the same as high HCO_3-Ringer's. In one series of experiments, several Cl concentrations were tested by substituting 0.5 mmol each of SO_4 and mannitol for each mmol of Cl. In all experiments, glucose (5–20 μmol/ml) was added to the serosal bathing medium and an equimolar amount of mannitol was added to the mucosal medium. The solutions were maintained at 15–16 °C and gassed with 1% CO_2 in O_2, the low CO_2 concentration having been selected to approximate the normally low ambient pCO_2 of fish. Under these conditions, the pH of high HCO_3 Ringer's was 8.2, and that of low HCO_3 Ringer's was 7.6.

Transmural PD, resistance, and short-circuit current (*Isc*) were measured as previously described [12]. Corrections were made for the resistance of the Ringer's solution between the tissue surfaces and the tips of the PD sensing bridges. The resistance of the Ringer's solution measured before mounting tissue was reduced by 10% to account for the displacement of some fluid by the mucosa, which weighed from 40 to 60 mg/cm^2.

Twenty to 60 min after tissues were mounted, ^{22}Na and ^{36}Cl (both New England Nuclear, Boston) were added to one reservoir and the tissues were short-circuited. Unidirectional mucosa (*m*)-to-serosa (*s*), *s*-to-*m* and net fluxes (J_{ms}, J_{sm}, J_{net}) were determined from initial samples taken 20 min after adding radioisotopes and duplicate final samples taken 30 to 40 min thereafter [12]. In preliminary experiments it was established that steady-state rates of ^{22}Na and ^{36}Cl transfer from *m*-to-*s* and from *s*-to-*m* were attained within 20 min. It was also established that the PD and resistance of the mucosa were constant from about 4 cm below the stomach to about 4 cm above the anus, suggesting that ion transport does not vary over the length of intestine employed.

Statistical analyses were by Student's *t* test for paired or unpaired variates. Results are presented as means ± 1 SEM.

Morphological Studies

Intestine was fixed immediately upon removal from the animal or immediately after study in chambers. In the latter case, mucosa was mounted in a parafilm frame which could then be removed from the chamber and placed in fixative in a few seconds. To correlate functional states of the epithelium with corresponding morphological features such as open lateral spaces, osmium tetroxide was used because of evidence [31] that aldehyde fixatives cause cell swelling and/or shrinkage. For these correlative studies tissues were fixed for 2–4 hr at 0–5 °C with 1% osmium tetroxide in pH 7.4 phosphate buffer containing 0.5 mM $CaCl_2$ [32]. For ultrastructural studies, tissues were fixed for 2–4 hr in either 6% glutaraldehyde in 0.2 M cacodylate buffer at pH 7.4 [19] or in a mixture of 1% acrolein, 1% formaldehyde, and 1% glutaraldehyde in 0.2 M phosphate buffer at pH 7.4 [40] and then postfixed for 90 min at 0–5 °C in phosphate-buffered 1% osmium tetroxide. To enhance membrane contrast in tight junctions, some tissues were fixed with 6% glutaraldehyde as described above and then postfixed with 1% OsO_4 containing 15 mg/ml of potassium ferricyanide [44]. In two experiments, lanthanum salts were added to conventional fixing solutions to provide an electron-dense precipitate in the extracellular spaces of the tissue [37]: Intestinal mucosa was fastened mucosal side up over the open end of a 0.5-cm diameter glass tube. Equal volumes of 4% aqueous $La(NO_3)_3$, pH 7.8, and 0.2 M cacodylate buffer, pH 7.4 (stock solution) were added to the tube (serosal side of the tissue), and also to a beaker into which the tube was placed (mucosal side). Sucrose was added to the beaker to 20% concentration in order to induce bulk flow of lanthanum across the epithelium. This sucrose gradient was maintained up to the dehydration step. Following overnight fixation in stock solution containing 3% glutaraldehyde (both sides of epithelium exposed), tissues were washed for 2 hr in stock solution containing 7.5% sucrose and postfixed for 3 hr in cold stock solution containing 1% OsO_4.

After three quick rinses in cold tap water, fixed tissues were rapidly dehydrated with increasing concentrations of ethanol and then embedded in Epon 812 [26] or Spurr low-viscosity epoxy resin (Polysciences, Inc., Worrington, Pa.). Sections for light microscopy (0.8–1.2 μm) were cut with glass knives and stained with methylene blue and Azure II [39]. Thin sections (500–800 A) were cut with a diamond knife, stained for 15 min with uranyl acetate, adjusted to pH 5 with 1 N NaOH, washed in distilled water, and counterstained for 15 min with lead citrate [38]. The thin sections were examined with a Hitachi HU-11C electron microscope operated at 75 Kv.

The percent area of the intestinal epithelium exhibiting distended lateral spaces was estimated from 1-μm plastic sections. The microscope was equipped with an ocular grid divided into squares which, at the magnification employed for this estimate, were 10 μm on a side. Estimates were made only from regions where the entire longitudinal profiles of the cells from the basal lamina to the intestinal lumen were visible.

Results

Physiological Studies

Electrical and flux measurements in high and low HCO_3 Ringer's solutions. When flounder intestinal mucosa was bathed in 20 mM HCO_3-containing Ringer's solution, bubbled with 1% CO_2 in O_2 and maintained at 15–16° (pH 8.2), the transmural PD was from 3 to 7 mV, serosa-negative. This PD remained stable for at least 3 hr. When bathed in 5 mM HCO_3-containing Ringer's solution (pH 7.6), the PD was appreciably lower, although still serosa-negative. At both HCO_3 concentrations, the electrical conductance (G_t) was between 20 and 40 mmhos/cm^2, which is similar to that of mammalian small intestinal mucosa [12, 34, 42].

Measurements of Na and Cl fluxes across the short-circuited mucosa are given in Table 1. Both Na and Cl were absorbed under short-circuit condition, but Cl absorption predominated: in 20 mM HCO_3-Ringer's, J^{Cl}_{net} was nearly three times J^{Na}_{net} and the difference between them was approximately equal to the *Isc*. J^{Cl}_{sm} and the ratio of J^{Cl}_{sm} to J^{Na}_{sm} were unusually low in comparison to the values reported for mammalian small intestine [12, 34, 42] and gall bladder [13].

Cl absorption and *Isc* were appreciably greater in the more alkaline medium. This is consistent with the report of Oide [35] that the intestine of the Japanese eel absorbs fluid far more rapidly from an alkaline (pH 9.0) than from a neutral (pH 7.2) solution and with the subsequent report by Hirano, Morisawa, Ando and Utida [21] that the serosa negativity of eel intestine in the Ussing chamber increases as pH is increased from 7 to 9. It is also consistent with the known stimulatory effect of HCO_3 on NaCl absorption by gall bladder [29]. Although the

Table 1. Na and Cl fluxes across the short-circuited intestinal mucosa of the flounder

Medium [HCO_3]	n	J^{Na}_{ms}	J^{Na}_{sm}	J^{Na}_{net}	J^{Cl}_{ms}	J^{Cl}_{sm}	J^{Cl}_{net}	I_{sc}	G
5 mM (pH 7.6)	7	12.1 ±0.787	10.7 ±0.711	1.35 ±0.590	4.99 ±0.630	2.97 ±0.317	2.02 ±0.646	−1.33 ±0.163	18.4 ±1.01
20 mM (pH 8.2)	13	13.6 ±0.746	11.6 ±0.794	1.96 ±0.288	8.43[a] ±0.494	2.97 ±0.332	5.46[a] ±0.401	−3.40[a] ±0.247	22.3 ±1.24

Values are means ±1 SE for n experiments; fluxes and I_{sc} are in μeq/hr cm^2 and conductance (G) is in mmhos/cm^2.

[a] Different from flux in 5 mM HCO_3-Ringer's, $P < 0.001$.

mean values for J^{Na}_{net} were not significantly different in the two Ringer's solutions, their magnitudes were too small relative to the unidirectional fluxes to be accurately measured in a small number of experiments. J^{Na}_{net} can, however, be indirectly estimated from the more accurately measured *Isc* and J^{Cl}_{net} by assuming that the *Isc* is equal to the difference between J^{Na}_{net} and J^{Cl}_{net} (even in high HCO_3 Ringer's, where some HCO_3 transport might have been expected, the *Isc* is wholly accounted for by the measured net fluxes of Na and Cl). This assumption gives values for J^{Na}_{net} of 0.69 and 2.06, respectively, suggesting that, whereas HCO_3 concentration (or pH) influences the magnitudes of the net fluxes, it does not affect the ratio of one to the other.

Interdependence of Na and Cl transport processes. In order to test for coupling between Na and Cl transport processes, we determined Cl fluxes in Na-free, Choline Ringer's and Na fluxes in Cl-free, SO_4-Ringer's. In both solutions (which also contained 20 mM HCO_3) the steady-state transmural PD was zero. The PD across tissues mounted in SO_4-Ringer's fell to zero within 10 min. In choline Ringer's, the PD, although it was initially 10 to 15 mV serosa-negative, fell within 30 min to less than 1 mV. When choline and SO_4 Ringer's solutions were replaced with NaCl Ringer's 90 min after tissues were mounted, the PD returned to its usual serosa-negative level, indicating that the tissues had remained viable. Steady-state Na and Cl fluxes in Na-free and Cl-free Ringer's solutions are given in Table 2. It can be seen that Na replacement with choline abolished J^{Cl}_{net} and Cl replacement with SO_4 abolished J^{Na}_{net}. In Choline Ringer's J^{Cl}_{sm} was twice as high as in Na-Ringer's, suggesting an increase in passive Cl permeability. As might be expected from the cation-selectivity of the mucosa, G_t was markedly reduced by

Table 2. Interdependence of Na and Cl fluxes

Solution	J^{Na}_{ms}	J^{Na}_{sm}	J^{Na}_{net}	J^{Cl}_{ms}	J^{Cl}_{sm}	J^{Cl}_{net}	I_{sc}	G
Na-free (11)	–	–	–	6.32	6.15[a]	0.17[a]	−0.16[a]	8.54[a]
	–	–	–	±1.91	±0.863	±0.655	±0.041	±0.696
Cl-free (8)	13.8	13.9	−0.11[a]	–	–	–	0.04[a]	17.1[a]
	±0.552	±0.747	±0.342	–	–	–	±0.030	±0.564

All solutions contained 20 mM HCO_3; Na was replaced by choline and Cl by SO_4 (75 mM) and mannitol (75 mM). Final measured Na and Cl concentrations in Na-free and Cl-free solutions were less than 1 mM.

[a] Significantly different from control values in Table 1, $P < 0.01$.

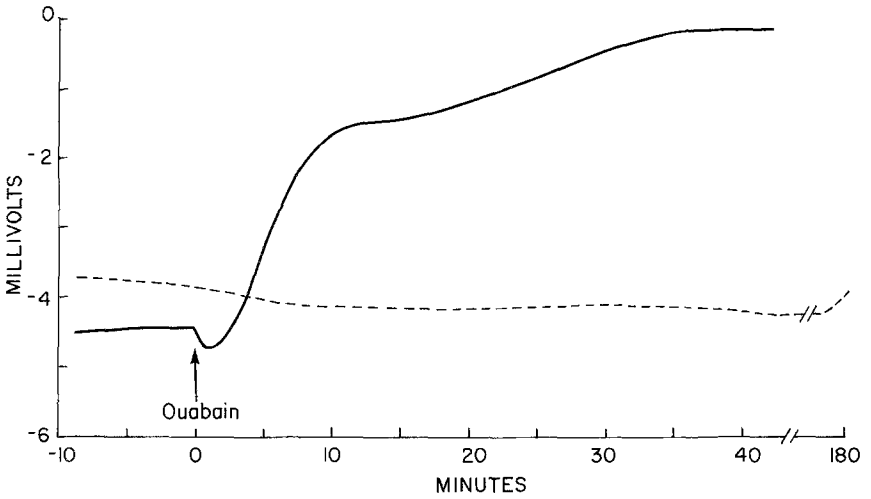

Fig. 1. Time course of change in PD across flounder intestinal mucosa bathed in high-HCO_3 Ringer's at 15°C. Ouabain (0.5 μmol/ml) was added to the serosal side at time zero. The dashed line represents a control tissue from the same fish. Results are representative of 11 experiments with and 40 without ouabain

Na replacement with choline but was only slightly reduced by Cl replacement with SO_4.

To further explore the coupling between Na and Cl transport processes, we examined the effects of ouabain. As shown in Fig. 1, the transmural PD was abolished by addition of ouabain (0.5 μmol/ml) to the serosal bathing medium. To ascertain that ouabain also abolished the net Cl flux, unidirectional Cl fluxes were measured: in 2 experiments mean values for J_{ms}^{Cl} and J_{sm}^{Cl} were 11.34 and 11.71, respectively.[1] Since the *Isc* was zero, we presume that the net Na flux was also abolished.

Effects of transmural PD and Cl concentration on J_{sm}^{Cl}. In order to provide a quantitative solution of the model for Na and Cl absorption presented below (*see Discussion*), we assumed that J_{sm}^{Na} and J_{sm}^{Cl} resulted exclusively from diffusion over the paracellular shunt pathway. This seemed a safe assumption for Na, in view of the large magnitude of J_{sm}^{Na} and the generally observed low permeability of basolateral membranes to Na. The variation of J_{sm}^{Na} with transmural PD had previously been evaluated by Nellans, Frizzell and Schultz [34] for nonsecreting rabbit

1 We have no explanation for the surprising increase in ${}_{o}J_{sm}^{Cl}$ caused by ouabain. Although the data here are for only 2 experiments, the same result was obtained in a larger series of experiments to be reported elsewhere (*see* footnote 3).

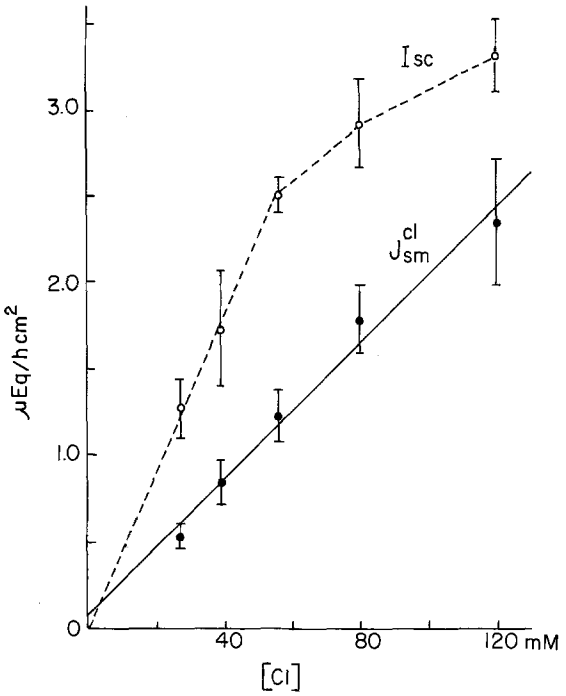

Fig. 2. Variation of ${}_oJ_{sm}^{Cl}$ and *Isc* with [Cl]. Equimolar amounts of SO_4 and mannitol were substituted for Cl. Results are means ±1 SE for 7 fish with all Cl concentrations tested on each fish and 1 or 2 concentrations on each tissue. The line was drawn by the method of least squares. The *Y*-intercept is not significantly different from zero

ileum and found to be wholly consistent with simple diffusion across a single membrane.[2] The assumption that J_{sm}^{Cl} is strictly paracellular seemed less secure, however, since its magnitude was small, and since epithelial cells may exhibit appreciable permeability to Cl. In rabbit gallbladder, for example, 2.2 μmol/hr cm² has been attributed to exchange diffusion [13]. We therefore evaluated J_{sm}^{Cl} in flounder intestine at different extracellular Cl concentrations and at different applied transmural PDs. Figure 2 shows the effect of [Cl] on J_{sm}^{Cl} and on *Isc*. Over the range 27 to 120 mM, J_{sm}^{Cl} varied linearly with [Cl], and the least squares regression line intercepts the *Y* axis at a point not significantly different from zero. Over the same range of [Cl], the *Isc*, which should be proportional to J_{net}^{Cl}, approaches saturation.

2 In a study by Dejeaux, Tai and Curran [10], J_{sm}^{Na} across rabbit ileal mucosa was found to have a PD-independent component. The differences between these two studies is probably due to the different HCO_3 concentrations employed. The higher HCO_3 concentration used by Desjeaux *et al.* results in active HCO_3 secretion which appears to be Na-coupled [42].

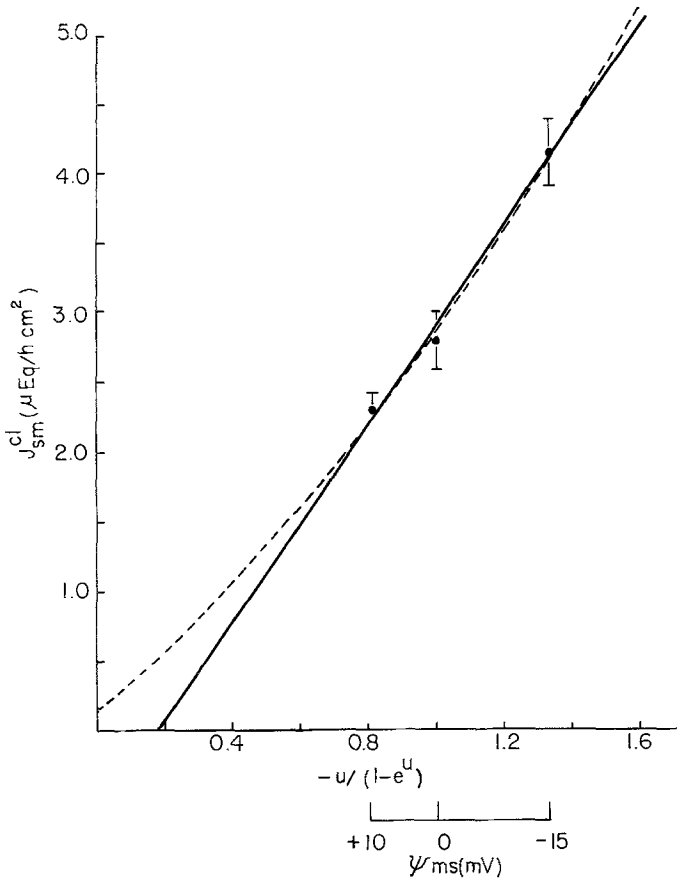

Fig. 3. Effect of PD on J^{Cl}_{sm}. $\mu=(F/RT)\times\Psi_{ms}$. Each tissue was clamped at 0 mV (short circuited) and also at either +10 or −15 mV (mucosal reference), clamping order being randomized. To reduce the effect of tissue variability, fluxes measured at +10 or −15 mV were normalized against fluxes measured at 0 mV: each of the fluxes measured at +10 or −15 mV was divided by the flux measured in the same tissue at 0 mV and multiplied by the group mean for J^{Cl}_{sm} at 0 mV. Results are means ±1 SE for 27 experiments at PD=ϕ and for 13 and 14 experiments at +10 and −15 mV, respectively. The solid line, drawn by the method of least squares, intercepts the *Y*-axis at a point not significantly different from zero. The dashed line is that predicted by the model in Fig. 11

The effects of 3 imposed PDs on J^{Cl}_{sm} are shown in Fig. 3. J^{Cl}_{sm} has been plotted against $-\mu/(1-e^{\mu})$ where $\mu=(F/RT)\times\Psi_{ms}$, F, R, and T have their usual meanings and Ψ_{ms} is the transmural PD. A linear relationship would suggest a simple diffusive flux across a single membrane, the magnitude of which is equal to the slope, and a positive *Y*-intercept would suggest a PD-independent, and therefore presumably transcellular

component of J_{sm}^{Cl} [41]. The straight line, which has been drawn by the method of least squares, intercepts the Y axis at a point not significantly different from zero. The curved line is that predicted by the model presented below for diffusion across two membranes in series (*see Discussion*). Both methods of analysis are consistent with a strictly paracellular route for J_{sm}^{Cl}.

Since large direct currents ($>320\,\mu A/cm^2$) alter the resistance of gallbladder [5] and might thereby affect J_{sm}^{Cl}, we also determined the conductances of the tissues used for measuring the effect of PD on J_{sm}^{Cl}. Values for current passed at $+10$, 0, and -15 mV were 268 ± 14, 76 ± 6 and $-223\pm16\,\mu A/cm^2$, respectively. Values for conductances at these PDs were 19.6 ± 1.0, 19.1 ± 0.8, and 20.9 ± 0.9 mmhos/cm^2, respectively. The small difference between the latter two values is significant ($P<0.001$).

Morphological Studies

Light Microscopy. The histology of flounder intestine (Fig. 4) conforms to the general pattern observed in a number of teleost species [8, 9, 16, 24, 49]. In human small intestine the absorptive surface is increased

Fig. 4. Light micrograph of flounder intestine. Note the absence of crypts of Lieberkuhn (42×)

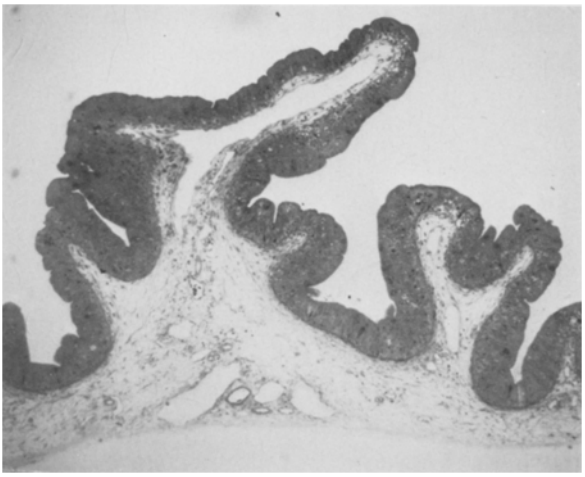

Fig. 5. Light micrograph of intestine (same segment as in Fig. 4) stripped of serosa and muscularis externa and mounted in a chamber. The mucosal folds are wider than in Fig. 4 due to stretching. (70×)

by a combination of plications and secondary, finger-like villi [47]. In flounder intestine large plications are not present but the mucosa is thrown into small folds which flatten considerably when the muscularis is removed and the mucosa is stretched onto a chamber (Fig. 5).

Another striking difference between flounder and mammalian intestine is the complete absence of crypts of Lieberkuhn in the former. Since these crypts have been postulated to be the source of active secretion in mammalian small intestine [20], it was of interest to determine whether cAMP, which stimulates secretion in mammalian intestine, would do so in flounder intestine. As we describe elsewhere[3], cAMP inhibits NaCl absorption in flounder intestine but does not stimulate secretion.

Interspersed within the simple columnar epithelium, which rests on a basal lamina, are scattered mucous cells, basal cells, which contain secretory droplets and are therefore probably endocrine in nature, and occasional small lymphocytes (Fig. 6). The absorptive cells are long (60 μm) and narrow (3.5 μm), and their nuclei are basal in location. Cells appear similar whether located at the tip or at the bottom of mucosal folds, e.g., the brush border seems equally well developed everywhere,

3 Field, M., Smith, P.L., Bolton, J.E. Ion transport across the isolated intestinal mucosa of the winter flounder, *Pseudopleuronectes americanus*. II. Effects of cyclic AMP *(submitted for publication)*.

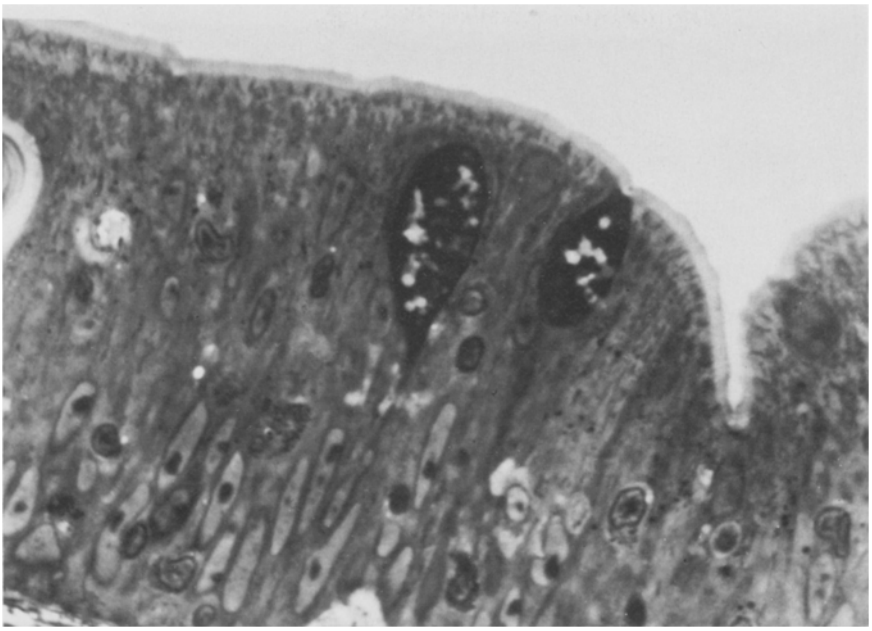

Fig. 6. Light micrograph of flounder intestinal epithelium, consisting predominantly of tall, narrow absorptive cells with elongated basal nuclei. Prominent terminal bars in the apical cytoplasm mark the boundaries of adjacent cells at their luminal poles. The granular appearance of the apical cytoplasm is due mainly to the large population of mitochondria in this region. (1380×)

and there is no evidence that cells found in the bottom of folds are less mature. Mitotic figures were not found, and it is therefore not apparent where epithelial cell renewal begins.

Distension of lateral spaces was consistently observed in transporting tissues (Fig. 7). The distended spaces were constricted at one or more points, probably due to desmosomes (*see below*). Distension rarely extended into the apical 12 μm of the lateral spaces. The fractional area of epithelium with distended spaces varied from tissue block to tissue block (34 to 92%) with an average of $53 \pm 10\%$ SE (observations were made from a total of 5 blocks from three fish as described under *Materials and Methods*). Distension was most prevalent between epithelial cells located at the tips of folds. No lateral space distension developed in 2 tissues exposed to ouabain (0.5 mM) for 40 min.

Electron Microscopy. The fine structure of flounder intestine absorptive cells (Figs. 8–10) is similar to that described for three fresh water

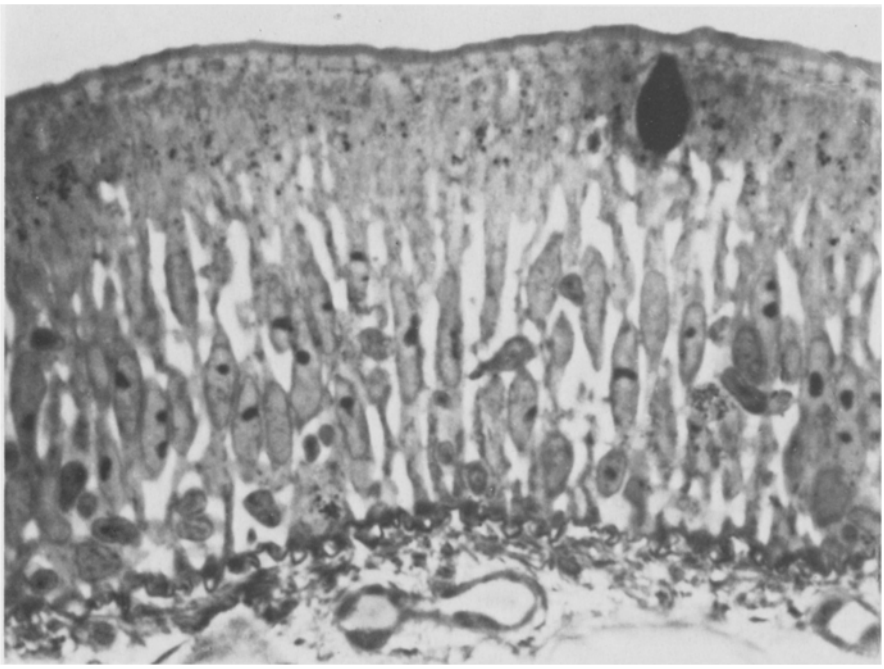

Fig. 7. Light micrograph of flounder intestinal epithelium which had been stripped, mounted, and perfused in an Ussing chamber for 60 min. Distension of lateral spaces with fluid is evident. (1300×)

species [24, 49]. The luminal surface exhibits a well-developed brush border about 1.0 μm thick. Mitochondria are scattered throughout the cytoplasm but are most dense in the apical and basal regions. A Golgi complex is located in the supranuclear region.

Absorptive cells are attached to each other at their apical poles by the typical junctional complex (*zonula occludens*, *zonula adherens*, and desmosome). The *zonula occludens* could not be demonstrated with conventional fixation but was clearly demonstrated in tissues prepared with the potassium ferricyanide procedure.[4] Desmosomes can be found along the full length of the cells, including the basal region. These cell-to-cell attachments, which restrict the separation of lateral surfaces, are especially common in the region of the nuclei (Fig. 9). A comparison with electron micrographs of mammalian intestinal absorptive cells [7, 45, 47] suggests that desmosomes beneath the junctional complex are more frequent in the flounder.

4 It would be of interest to reexamine with this procedure the two tissues in which the *zonula occludens* has been reported not to be present: nasal salt gland [28] and elasmobranch rectal gland [48].

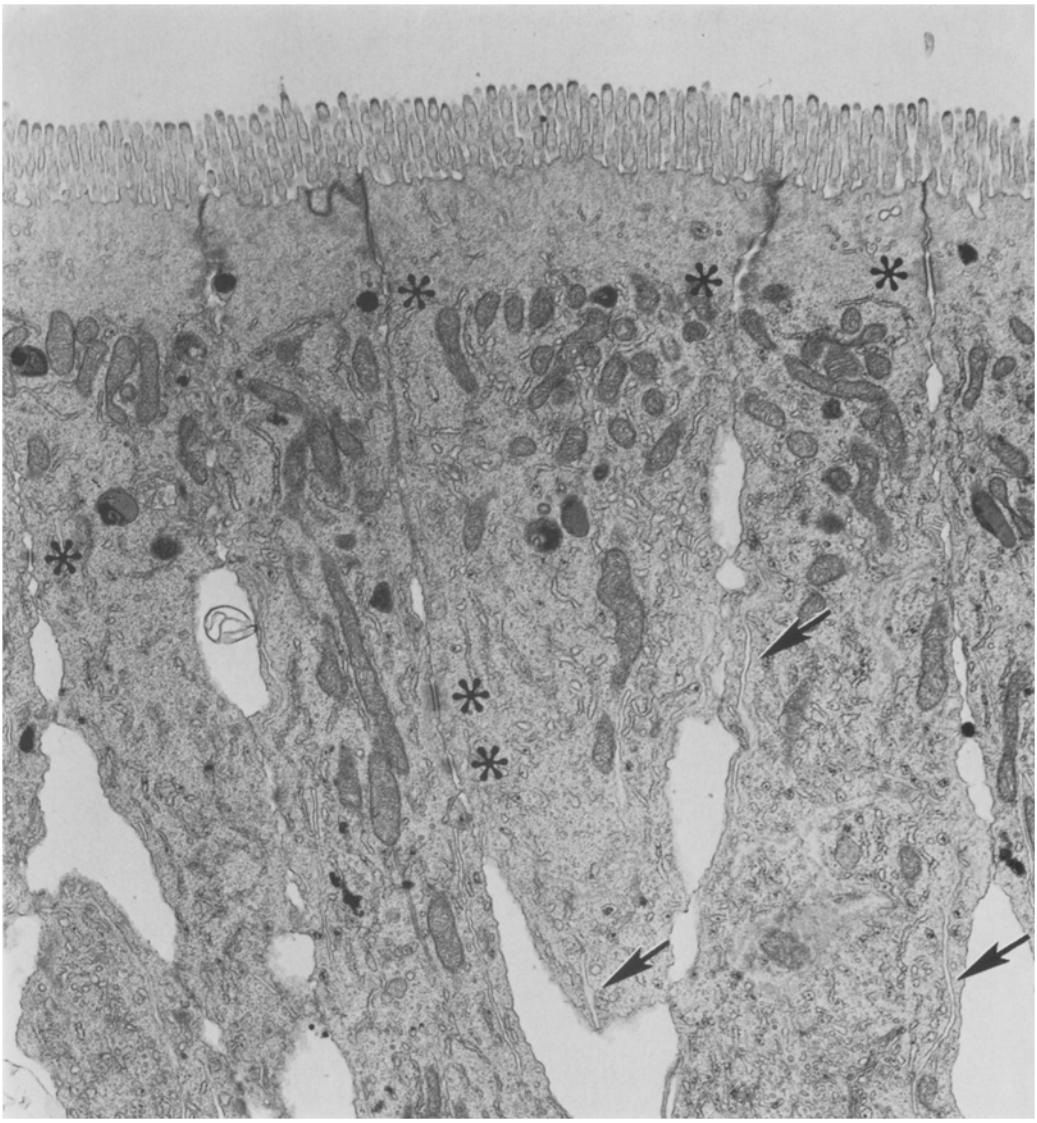

Fig. 8. Electron micrograph of the apical region of flounder intestinal epithelium, showing several absorptive cells. From the apex towards the base, there are, in succession, a brush border, a terminal web region, and a region of mitochondria with scattered elements of rough endoplasmic reticulum. Desmosomes, which restrict the distension of intercellular spaces, are found along the lateral plasma membrane (asterisks). Several examples of lateral infoldings are shown at the arrows. (16,000 ×)

The rarity of lateral space distension in the apical region, which is evident in the light micrograph (Fig. 7), is also seen in the electron micrograph of this region (Fig. 8), although intermittent small dilitations

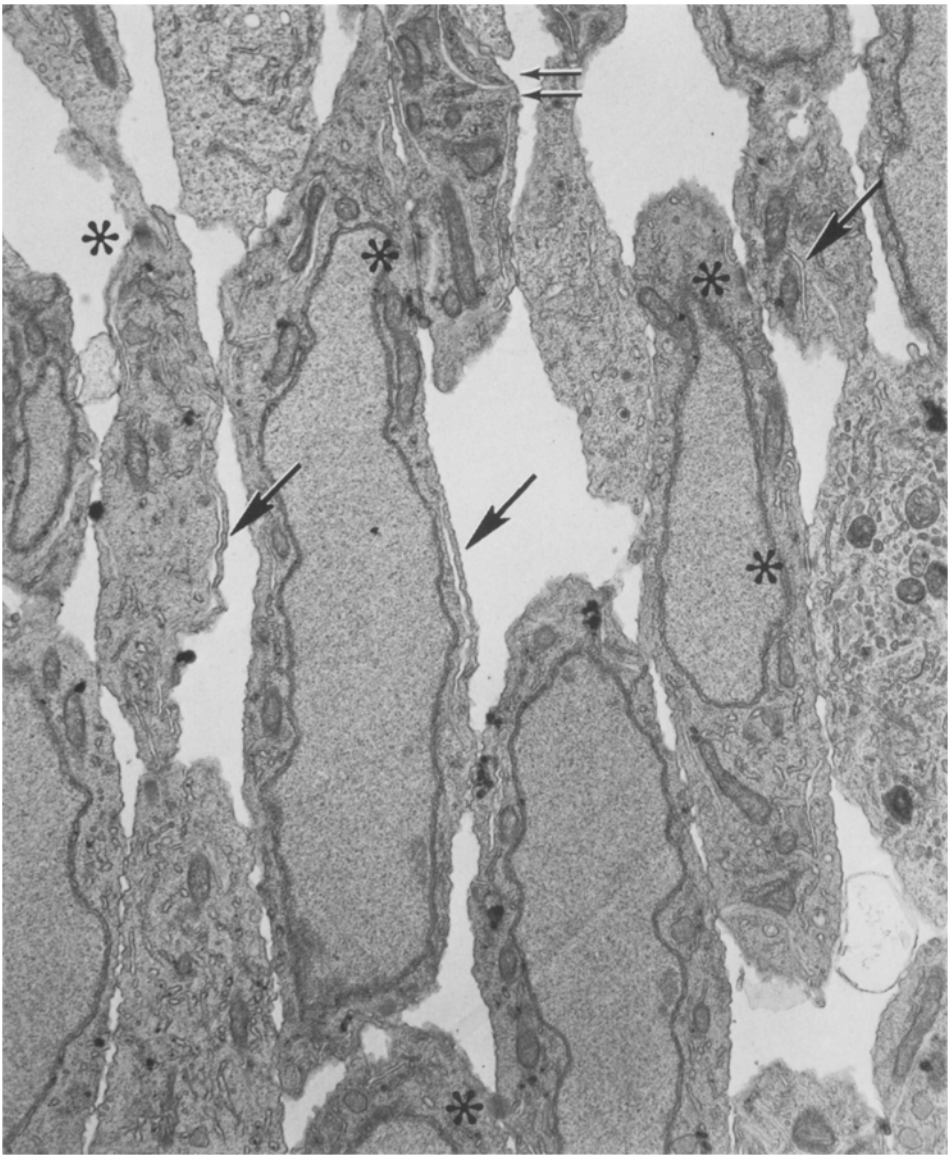

Fig. 9. Electron micrograph of flounder intestinal epithelium cut at the level of the nuclei. Numerous absorptive cells have been caught in tangential section. Desmosomes are found frequently along the lateral plasma membranes (asterisks). Lamellar structure to the lateral plasma membrane is shown at the double arrow. (16,000 ×)

are clearly present. Lateral space segments of diameter too small to measure are frequent.

The lateral surface of the absorptive cell is amplified by surface infolding, rather than by the lateral interdigitations found in mammalian

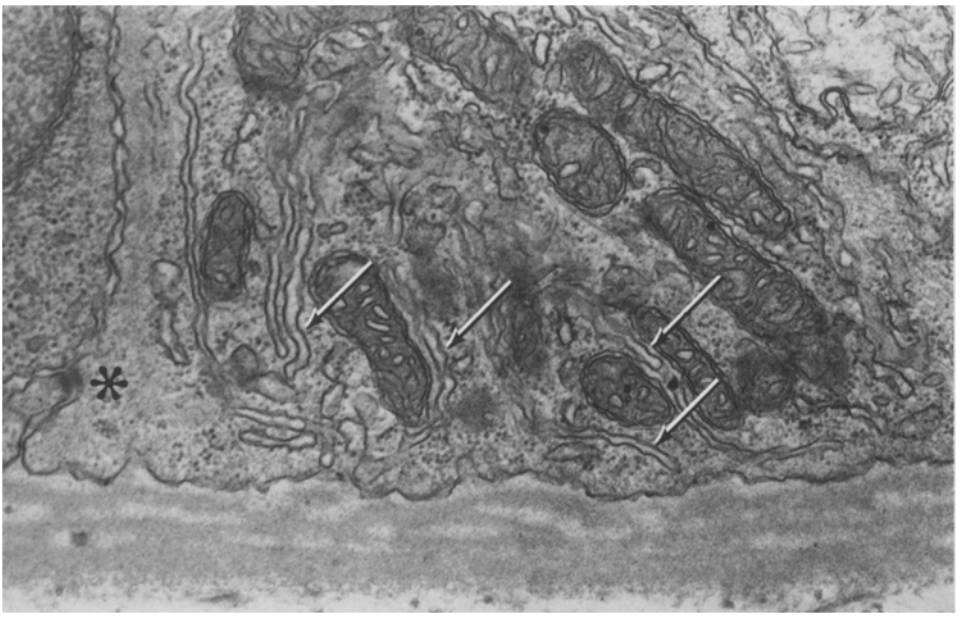

Fig. 10. Electron micrograph of flounder intestinal epithelium, showing the basal portion of an absorptive cell. The cytoplasm contains many lamellar structures (arrows) and mitochondria. A desmosome is seen on the far left (asterisk). The basal lamina is shown at the bottom. (28,700 ×)

intestine [47]. Connections between these lamellar structures and the lateral plasma membrane are seen clearly in Fig. 9. Connections between lamellar structures in the basal region and the basal plasma membrane were not observed, but it is possible that more extensive search of thin sections would have revealed such connections. Further evidence that these lamellar structures represent extensions of lateral (and possibly the basal) cell surface was obtained with the electron-opaque extracellular marker, lanthanum, which penetrated into the folds at all levels of the cytoplasm (photomicrograph not shown but can be obtained from the authors upon request).

Discussion

Relation between Na and Cl Transport Processes in Teleost Intestine

In mammalian [14, 33, 34] and amphibian [36] small intestine and in both teleost [11] and mammalian [13] gallbladder, there is considerable evidence that the Na gradient is the driving force for "active" Cl

absorption and that the site of direct coupling between Na and Cl movements is at the luminal border of the epithelial cells. First, a saturable portion of the influx of Cl across the luminal border of rabbit ileum [33] and gallbladder [13] is coupled one-for-one to the influx of Na. Removal of Na decreases Cl influx and abolishes net Cl transport and removal of Cl causes an equal decrease in Na influx and either diminishes (intestine) or abolishes (gallbladder) net Na transport. Second, measurements of intracellular electric potential and exchangeable Cl concentration suggest that Cl accumulates in these absorptive cells above electrochemical equilibrium [13, 14]. Cl entry from the luminal solution appears to be uphill and Cl exit into the serosal solution, downhill. When Na is omitted from the bathing medium the intracellular exchangeable Cl concentration declines towards the expected value for passive distribution. Finally, in both small intestine (R.T. Schooley and M. Field, *unpublished*) and gallbladder [30], ouabain, whose action appears to be confined to the inhibition of Na, K-ATPase, abolishes not only net Na absorption, but also net Cl absorption.

This model for active Cl absorption can also explain satisfactorily the observations of House and Green [22] on the marine teleost, *Cottus scorpius:* The PD was nearly zero despite a high rate of NaCl absorption, Cl absorption was abolished when Na was replaced with choline, and Na absorption was reduced by 80% when most of the Cl (13 mM remaining) was replaced with SO_4. In contrast, prior observations on the flounder [23, 43], on the eel [1, 2, 21], and on three additional species of marine teleosts [2] have given rise to a different explanation for Cl absorption, namely, a Na-independent, electrogenic Cl pump. When intestine from these marine teleosts was bathed on both sides with identical NaCl Ringer's solutions, the transmural PD was serosa-negative. When most of the Na was replaced with choline or tetraethyl ammonium, serosa-negativity persisted [23] or even increased [2, 21], and when most of the Cl was replaced with SO_4, the PD became serosa-positive [2, 23]. Furthermore, under short-circuit condition, the net flux of Cl across eel intestine was found by Ando *et al.* [2] to be twice as large as the net flux of Na. Finally, Smith *et al.* [43] found in the European flounder that the initial rate of uptake of ^{36}Cl across the luminal border remained constant as Na concentration was varied from 120 to 30 mM and actually increased when all Na was replaced with choline.

While the present study confirms prior observations on flounder and eel intestine with respect to the serosa-negative PD and the predominance of J^{Cl}_{net} over J^{Na}_{net} under short-circuit condition, it appears to con-

tradict prior observations on the effects of ionic substitutions. Careful scrutiny of these prior studies suggests, however, that the stated differences are more apparent than real.

With regard to the Na dependence of Cl transport, it should be noted that the choline Ringer's solutions employed by both Huang and Chen [23] and Ando *et al.* [2] contained 25 mM Na ($NaHCO_3$ was not replaced with choline HCO_3) and therefore may have sustained a substantial rate of coupled NaCl transport. For example, if the kinetic constants for coupled NaCl influx across the brush border of rabbit ileum [33] are applied to the experiments of Huang and Chen [23], the calculated coupled NaCl influx in their choline Cl Ringer's (25 mM Na, 120 mM Cl) is 53% of the rate calculated for their NaCl-Ringer's (140 mM Na, 120 mM Cl). It is therefore interesting that Huang and Chen [23] found J_{net}^{Cl} in their choline Cl Ringer's to be 47% of J_{net}^{Cl} in their NaCl Ringer's.

The markedly negative values for PD and *Isc* observed by Ando *et al.* [2] in choline Cl-Ringer's also cannot be regarded as proof that Cl transport is independent of Na. These tissues were clearly not in steady state since the PD steadily fell over the 50 min for which measurements are shown [21]; furthermore, if these measurements of *Isc* really reflect net Cl absorption, then J_{net}^{Cl} would have been 3 to 4 times greater in choline Ringer's than in Na Ringer's, which seems unlikely. It is more likely that these PDs resulted from asymmetric diffusion potentials at the two sides of the tissue created by slow exchanges of Na in the tissue for choline in the medium. In our preparation of stripped flounder intestine, a stable zero PD in choline Cl Ringer's does not develop for 30–40 min. The approach to steady-state may be still slower in unstripped eel intestine because of its thick muscle layer.

Finally, the measurements by Smith *et al.* [43] of Cl uptake across the mucosal border of flounder intestine are not sufficiently definitive to exclude coupled NaCl influx. As shown in Table 2 of the present study, J_{sm}^{Cl} doubled when Na was replaced by choline, suggesting an increase in passive Cl permeability. This could be the explanation for the paradoxical increase in Cl influx that Smith *et al.* [43] observed in Na-free choline Ringer's. Furthermore, if the kinetic constants for Na-coupled Cl influx into rabbit ileum [33] are also applicable to flounder intestine, only a 36% change in coupled influx would be expected over the concentration range employed by Smith *et al.* [43] (aside from experiments at 0 mM Na). It is doubtful whether this small a difference could be established in a small number of experiments. Our own recently acquired data on Na

and Cl uptake across the luminal border of intestine from the winter flounder indicates the presence of a coupled influx process of sufficient magnitude to explain the net Cl flux.[5]

With regard to the Cl-dependence of Na transport, it is worth noting that, in the studies of marine teleost intestine cited above (but not in the present study), glucose was present in the mucosal bathing medium. Thus, in these studies some cotransport of glucose and Na would be expected and may account for the presence of a serosa-positive PD in Na_2SO_4-Ringer's. These studies do not exclude the possibility that there is also a Cl-dependent component of transmural Na transport. Indeed, the only prior measurements of J_{net}^{Na} at both high and low Cl concentrations were those of House and Green [22] on *Cottus scorpius* in which more than 80% of J_{net}^{Na} was found to be Cl-dependent.

In summary, review of prior studies indicates that, despite their authors' interpretations, the data shown are not inconsistent with the present findings, which suggest that Cl transport across teleost intestine is coupled to that of Na and is driven by the Na gradient. More experimental data are needed before this conclusion can be accepted as proven. In particular, it will be necessary to determine the electrochemical potential of Cl in the intestinal epithelial cells.

The Lateral Intercellular Space Considered as a Tissue Compartment: Its Possible Role in Generation of the Transmural PD and in Salt Absorption

If net Cl absorption by flounder intestine results from a 1:1 Na-coupled influx and the Na gradient (as appears to be the case in rabbit gallbladder [13] and ileum [33]), then the intestinal cells cannot transport more Cl into the lateral space than Na (depending on the relative permeabilities to Cl of basolateral and brush border membranes, these cells may transport less Cl than Na). If we accept this mechanism for Cl absorption, how can we explain the serosa-negative PD and the preponderance of J_{net}^{Cl} over J_{net}^{Na} when the tissue is short-circuited? This paradox becomes explicable once we consider that transcellular fluxes may differ significantly from transepithelial fluxes due to the permselective and resistive properties of the paracellular shunt pathway.

5 Frizzell, R.A., Smith, P.L., Field, M. 1978. Coupled NaCl influx across brush border of winter flounder. *Fed. Proc.* **37**:513 (*abstr.*)

It seems likely from the relative magnitudes of J_{sm}^{Na} and J_{sm}^{Cl} in Table 1 that the paracellular pathway is highly cation-selective. The ratio of J_{sm}^{Na} to J_{sm}^{Cl} is in fact appreciably greater in flounder intestine than in either rabbit ileum [12, 34, 42] or rabbit gallbladder [13]. The site of cation selectivity is probably the tight junction, across which a NaCl diffusion potential should develop if active transport elevates the salt concentration in the lateral space above that in the bathing medium. A smaller diffusion potential should also develop along the lateral space since the mobility of Cl in free solution is about 50% greater than that of Na. Both diffusion potentials would contribute to the serosa-negativity of the transmural PD. Machen and Diamond [27] found the transmural PD of maximally transporting gallbladders to be 1.4 mV serosa-negative and used this value to estimate the average salt concentration in the lateral space (about 10 mM above that in the bathing medium). The larger magnitude of the serosa-negative PD (3–7 mV) in flounder intestine could result from greater cation selectivity in the tight junction or a higher salt concentration in the lateral space. The magnitude of the latter is determined in part by the resistances to ionic diffusion in luminal and contraluminal directions. Frömter [15] has suggested, on the basis of measurements with microelectrodes in *necturus* gallbladder, that the resistance in the lateral space becomes significant relative to junctional resistance when the space width falls below 0.1 μm. As can be seen from Fig. 8, narrow lateral space segments are common in the apical region of actively absorbing flounder intestinal epithelium.

These considerations about the origin of the transmural PD also have consequences for the relative rates of Na and Cl absorption across the short-circuited epithelium. Since the flounder intestinal epithelial cells are 60 μm long and only 3.5 μm wide, almost all transport from the cell to the serosal medium occurs by way of the lateral space (the ratio of lateral to basal surface area is approximately equal to twice the length divided by one-half the width or about 70:1). Under open-circuit condition, however, the requirement for electroneutrality is met by the external circuit and therefore Na and Cl are free to diffuse independently. If the resistance to Na diffusion in the lateral space is higher than that in the cation-selective tight junction, then, under short-circuit condition, most of the Na entering the pathway from the epithelial cells will diffuse back into the luminal bathing solution. This will be especially likely if most Na pump activity is concentrated near the apical end of the epithelial cell. Since, however, the Cl permeability of the tight junction appears to be relatively low, most of the Cl pumped into the lateral space

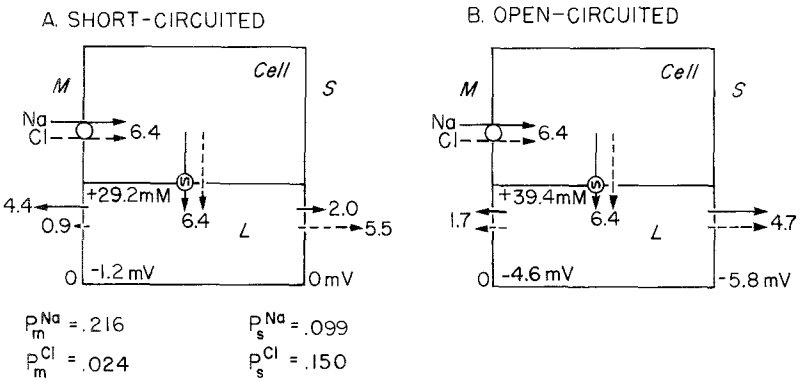

Fig. 11. Possible role of paracellular shunt pathway in altering transcellular NaCl fluxes in flounder intestine. Values for permeabilities (*P*) of the mucosal (*m*) and serosal (*s*) boundaries of the lateral space (*L*), fluxes across these boundaries and across the cell borders (indicated by solid arrows for Na and dashed arrows for Cl), and differences in salt concentration and electric potential in the lateral space have been calculated for short-circuited (*A*) and open-circuited (*B*) states. (*See text* for details)

will be transported in the contraluminal direction. Thus, under short-circuit condition, a marked difference between J_{net}^{Cl} and J_{net}^{Na} could arise.

In order to explore the quantitative implications of this argument, we have modelled the lateral space as a tissue compartment into which the cell transports NaCl and out of which these ions can diffuse into both mucosal and serosal bathing solutions (Fig. 11). The mucosal boundary of the lateral space can reasonably be equated with the tight junction. A comparably discrete anatomic counterpart of the serosal boundary does not appear to exist but a first approximation would be the overall resistance present in the lateral space distal to the tight junction.

To arrive at a unique solution of the model, using as input the flux data in Table 1 for 20 mM HCO_3-Ringer's, we need to make some assumptions:

(i) Na and Cl are the only ions for which there is net transepithelial transport. This assumption is not unreasonable since the *Isc* was equal to $J_{net}^{Na} - J_{net}^{Cl}$, implying no HCO_3 transport. Furthermore, there is no evidence for active transepithelial K transport in vertebrate intestine. Ca transport may be present but would be quantitatively insignificant relative to Na and Cl.

(ii) Na and Cl are both present in the bathing media at 150 mM concentration. This assumption, which simplifies calculations greatly, departs only slightly from the actual concentrations of Na (168 mM) and Cl (150 mM) employed.

It follows from *i* and *ii* that the concentrations of Na and Cl in the lateral space (L) must be equal, i.e.,

$$c_L^{Na} = c_L^{Cl} = c_L. \tag{1}$$

(iii) Net fluxes of Na and Cl across the m and s boundaries of L conform to the Goldman "constant field" equation [18], i.e.,

$$J_j^i = P_j^i Z^i \mu_j (c_L - c_0 e^{-Z^i \mu_j})/(1 - e^{-Z^i \mu_j}) \tag{2}$$

where i refers to Na or Cl, j to m or s, $\mu_j = (F/RT)(\Psi_L - \Psi_j)$ with $\Psi_m = \phi$, $c_0 = 150\,m$M and Z, F, R, and T have their usual meanings. Note that J_j^i is always positive if directed out of L, whether in the m or s direction.

Under short circuit condition, ${}_o\mu_m = {}_o\mu_s = {}_o\mu_L$. It therefore follows from Eq. (2) that

$$\frac{P_m^i}{P_s^i} = \frac{{}_oJ_m^i}{{}_oJ_s^i}, \tag{3}$$

the subscript o referring to the short-circuited state.

(iv) Na and Cl permeabilities at the serosal boundary of L relate to each other as do the free solution mobilities (M) of these ions, i.e.,

$$P_s^{Na} = R_m P_s^{Cl}, \quad \text{with } R_m = \frac{M(Na)}{M(Cl)} = 0.658. \tag{4}$$

If the expressions for ${}_oJ_s^{Na}$ and ${}_oJ_s^{Cl}$ derived from Eq. (2) are combined so as to eliminate ${}_oc_L$ and if P_s^{Na}/R_m is substituted for P_s^{Cl}, then P_s^{Na} can be defined as a function of ${}_o\mu_L$:

$$P_s^{Na} = \frac{{}_oJ_s^{Na} - {}_oJ_s^{Cl} e^{o\mu_L} R_m}{{}_o\mu_L c_0 (1 + e^{o\mu_L})}. \tag{5}$$

(v) J_{sm}^{Na} and J_{sm}^{Cl} are strictly paracellular, i.e., unidirectional fluxes of Na and Cl from L to cell (c) or from c to m are sufficiently low that

$$J_{sm}^i = J_{sL}^i J_{Lm}^i / (J_{Lm}^i + J_{Ls}^i). \tag{6}$$

Evidence in support of this assumption was presented earlier. Each of the unidirectional fluxes on the right side of Eq. (6) can be described by the Goldman equation with the trans-concentration set at zero, i.e.,

$$J_{sL}^i = P_s^i c_0 V_s^i e^{-Z^i \mu_s}) \tag{7.0}$$

$$J_{Lm}^i = P_m^i c_L V_m^i \tag{7.1}$$

$$J_{Ls}^i = P_s^i c_L V_s^i.$$

where

$$V_j^i = Z^i \mu_j / (1 - e^{-Z^i \mu_j}). \tag{7.2}$$

Substituting these expressions into Eq. (6) gives

$$J_{sm}^i = c_0 \frac{P_m^i V_m^i P_s^i V_s^i e^{-Z^i \mu_s}}{P_m^i V_m^i + P_s^i V_s^i} \tag{8}$$ [6]

Under short-circuit condition, $V_m^i = V_s^i$ and, therefore,

$${}_oJ_{sm}^i = c_0 \bar{P}_{sm}^i \frac{Z^i {}_o\mu_L}{e^{Z^i {}_o\mu_L} - 1} \tag{9}$$

where

$$\bar{P}_{sm}^i = \frac{P_m^i P_s^i}{P_m^i + P_s^i}.$$

Since the system is in steady-state,

$$J_m^i + J_s^i = J_c^i, \tag{10}$$

where J_c^i is the net flux of i from cell (c) to L. By combining Eqs. (3), (9) and (10), the following expressions for ${}_oJ_c^i$ can be obtained:

$${}_oJ_c^{Na} = \frac{{}_oJ_s^{Na}}{1 + {}_oJ_{sm}^{Na}(1 - e^{o\mu_L})/(c_0 P_s^{Na} {}_o\mu_L)} \tag{11.0}$$

and

$${}_oJ_c^{Cl} = \frac{{}_oJ_s^{Cl}}{1 - {}_oJ_{sm}^{Cl}(1 - e^{-o\mu_L}) R_m/(c_0 P_s^{Na} {}_o\mu_L)}. \tag{11.1}$$

(vi) Finally, both Na and Cl are transported at equal rates from c to L so that

$${}_oJ_c^{Na} = {}_oJ_c^{Cl}. \tag{12}$$

If the expression for P_s^{Na} in Eq. (5) is substituted into 11.0 and 11.1 and if the latter two equations are set equal to each other, then ${}_o\mu_L$ can be determined by successive approximations, using values from Table 1 for ${}_oJ_s^{Na} (= {}_oJ_{net}^{Cl})$, ${}_oJ_s^{Cl} (= {}_oJ_{net}^{Cl})$, ${}_oJ_{sm}^{Na}$ (after multiplying by 150/168 in order to adjust for an assumed medium [Na] of 150 mM) and ${}_oJ_{sm}^{Cl}$. Once ${}_o\mu_L$ is known, the correct values for ${}_oc_L$, ${}_o\Psi_L$, P_j^i, ${}_oJ_m^i$ and ${}_oJ_c^{NaCl}$ are easily obtained (*see* Fig. 11 *A*). The model predicts that P_m^{Na} is 9 times P_m^{Cl} and more than twice P_s^{Na} and, therefore, that about 70% of the Na entering

6 Equation (8) is essentially the same as that derived by Schultz and Frizzell [41].

the space diffuses back into the mucosal solution, whereas 85% of the Cl entering the space diffuses into the serosal solution. The model also predicts that under short-circuit condition the concentration of NaCl in the lateral space is 29 mM higher than in the bathing medium.

If we assume that short circuiting does not change either J_c^{NaCl} or P_j^i, then, by using Eqs. (2) and (10) and the open-circuit condition, $J_j^{Na} = J_j^{Cl}$, we can obtain the values for the open circuited state shown in Fig. 11*B*: the salt concentration in the lateral space is now 39 mM higher than in the bathing medium, Ψ_{ms} is -5.8 mV, and the NaCl fluxes into mucosal and serosal solutions are 1.7 and 4.7, respectively.[7] Although the predicted Ψ_{ms} is greater than that calculated from the values for I_{sc} and G_t in Table 1 (-3.8 mV), this difference appears to be due not to a failure of the model *per se* but to a discrepancy between the sum of the passive Na and Cl conductances (equal to $J_{sm}^{Na} + J_{sm}^{Cl}$) and the measured total conductance (G_t). Only a small portion of this discrepancy can be attributed to other ions in solution. Measurement of G_t may be affected by the magnitude and direction of current flow and by time transients. The model predicts a higher salt concentration in the lateral space under open-circuit than under short-circuit condition. Thus current flow may effect a redistribution of ions in the tissue that may, in turn, affect measurements of G_t. These ambiguities can only be resolved by a detailed study of the current-voltage relationship.

Several additional comments on this model seem pertinent:

(i) The calculated ratio for P_m^{Cl}/P_m^{Na} of 0.11 is precisely the same as the P^{Cl}/P^{Na} for rabbit gallbladder estimated by Barry, Diamond and Wright [4] from NaCl dilution potentials. Although these dilution potentials do not necessarily arise exclusively at the tight junction, it is likely that the junctional contribution to the overall ion selectivity of the epithelium is much greater in rabbit gallbladder than in flounder intestine since, despite comparable rates of ion transport, the transmural PD generated by active salt absorption is much smaller in the former [27] than in the latter tissue.

---

7 Since $J_j^{Na} = J_j^{Cl}$, it follows from Eq. (2) that

$$e^{\mu_m} = (P_m^{Cl} C_L + P_m^{Na} C_0)/(P_m^{Na} C_L + P_m^{Cl} C_0)$$

and

$$e^{\mu_s} = (P_s^{Cl} C_L + P_s^{Na} C_L)/(P_s^{Na} C_L + P_s^{Cl} C_0).$$

Furthermore, since the system is in a steady state [Eq. (12)],

$$J_C^{NaCl} = 6.4 = P_m^{Na} \mu_m (C_0 - C_L e^{\mu_m})/(1 - e^{\mu_m}) + P_s^{Na} \mu_s (C_0 - C_L e^{\mu_s})/(1 - e^{\mu_s})$$

C_L can be determined readily by successive approximations.

(ii) If J_{sm}^{Cl} represents simple diffusion across a single homogeneous membrane, it should vary linearly with the function $-\mu_{ms}/(1-e^{\mu_{ms}})$ [41]. If, however, J_{sm}^{Cl} represents simple diffusion across two membranes in series, the relation between these variables will be curvilinear [*see* Eq. (8)] and its *Y*-intercept will be higher than that predicted by the straight line which best fits the experimental points. Figure 3 shows the curve obtained with the PD-independent values shown in Fig. 11*A* after suitable corrections are made for small differences between the two sets of experiments (*see Appendix*). Both the straight line and the curve fit the experimental points reasonably well. While larger clamping voltages might be expected to distinguish between them, application of such voltages is probably not feasible since high current flows can produce major structural changes in the paracellular pathway [5].

(iii) As indicated earlier, if the Na gradient is the sole driving force for Cl absorption, then J_c^{Cl} cannot exceed J_c^{Na}. The values given in Fig. 11 apply to the condition $J_c^{Na}=J_c^{Cl}$. Even if $J_c^{Na}>J_c^{Cl}$, which would be the case if (a) some Cl crossing the brush border coupled to Na were to leak back into the luminal solution of if (b) some Na influx were Cl-independent, then the values in Table 1 could still be consistent with the model, although a still larger fraction of ${}_oJ_c^{Na}$ would necessarily recycle to the luminal side. If, for example, ${}_oJ_c^{Na}=1.5$ ${}_oJ_c^{Cl}$, then ${}_o\Psi_L=-1.4$ mV, ${}_oC_L=184.2$ mM, ${}_oJ_c^{Na}=9.8$, ${}_oJ_c^{Cl}=6.6$, $P_m^{Na}=0.331$, $P_m^{Cl}=0.0245$, and $P_s^{Na}=0.085$.

(iv) Marked changes in transmural PD and *Isc* of bullfrog small intestine are produced by changes in solution osmolality [3]. These electrical changes have been postulated by Armstrong [3] to result from changes in resistance or diffusion potential in the paracullular shunt pathway. Thus another line of evidence points to a major role for the paracellular pathway of "leaky" epithelia in modifying transcellular ion fluxes.

(v) This model obviously is not entirely realistic. Ion movements from lateral space to serosal medium may be largely convective and therefore not accurately described by a diffusion equation. The lateral space is not a well-stirred solution with uniform ion concentrations throughout and the serosal boundary to the space probably does not exist as a discrete barrier. Nonetheless, the fundamental conclusions from this analysis will not be contradicted by a more complex analysis of the data. In general, if lateral space resistances to ion movements are significant relative to junctional resistances, it becomes hazardous to extrapolate from transmural PD and flux measurements to transport

events at the cellular level. It follows that a serosa-negative PD and ${}_oJ^{Cl}_{net} > {}_oJ^{Na}_{net}$ are not by themselves sufficient evidence for the existence of an electrogenic (or rheogenic) Cl pump. A ouabain inhibitable, serosa-negative PD has also been noted in the thick ascending limb of Henle's loop in rat kidney [6]. It may be worthwhile to consider the interpretation offered here as an alternative to an electrogenic Cl pump at that site.

Correlation between Structure and Function

The above model for ion transport in flounder intestine can only be valid if the resistance to Na movement along the lateral space is greater than that in the tight junction. This can be the case if an appreciable portion of the lateral space remains narrow (0.1 μm) during active fluid absorption [15]. As can be seen in Fig. 6, lateral space segments with diameter well below 0.1 μm are evident in the apical portion of actively absorbing flounder intestinal epithelium. There is also a high density of mitochondria in this region, suggesting that much of the active ion transport activity of the cell occurs there. The importance of lateral space dimensions in determining tissue resistance is also suggested by Bindslev, Tormey and Wright [5], who correlated the changes in these variables produced by osmotic and electrical gradients. Induction of *m*-to-*s* volume flow dilated spaces and reduced resistance and vice versa for *s*-to-*m* volume flow.

In contrast to the pattern of lateral space distension during active salt absorption across the isolated intestinal mucosa of the flounder, lateral spaces in *in vitro* preparations of gallbladder distend up to the tight junction [5, 25, 46]. This difference from flounder intestine may be associated with lower salt concentrations in the apical portion of the lateral space and could account for the lower transmural PDs in gallbladder. In the gallbladder preparations cited above, muscle layers were not removed. It is well known that during fluid absorption *in vitro* across full thickness preparations of epithelial tissues, fluid tends to accumulate in the subepithelial space due probably to the hydraulic resistance presented by the muscle layer. This interstitial edema results in a build-up of hydrostatic pressure which is then transmitted into the lateral intercellular space. Interstitial pressure is probably far smaller in *in vitro* preparations stripped of muscle, such as the one we have employed. It is of interest in this regard that Kaye, Wheeler, Whitlock and Lane [25]

found less lateral space dilitation when rabbit gallbladder was perfused *in vivo* than when it was perfused *in vitro*, despite higher rates of fluid absorption *in vivo*.

Another factor which may contribute to these different patterns of lateral space distension is the greater frequency of desmosomes along the lateral membrane of flounder intestinal epithelial cells. The photomicrographs of mammalian [25, 46] and amphibian [5] gallbladder that we have been able to examine display relatively few desmosomes. These constrictions may serve to dampen the transmission of hydrostatic pressure from the subepithelial region to the apical portion of the lateral spaces.

We thank Mr. Harold Church for his excellent technical assistance with the morphological studies. We are indebted to James B. Wade (Yale University) for a helpful discussion on tight junction morphology and to Stanley G. Schultz (University of Pittsburgh) and William McD. Armstrong (University of Indiana) for their thoughtful criticisms of our manuscript. This investigation was supported by Public Health Service Grants AI-09029 (U.S.-Japan Cooperative Medical Science Program) and AM-18704 (both to Michael Field) and Health Service Grants AM-15973 (to William B. Kinter) and Fellowship GM-57244 (to Karl J. Karnaky, Jr.).

Appendix

Derivation of Curve in Figure 3

If the model in Fig. 11 is correct, then J_{sm}^{Cl} represents diffusion across 2 membranes in series and therefore it will not vary linearly with the function $-\mu_{ms}/(1-e^{\mu_{ms}})$, which is based on diffusion across a single membrane. The variation of J_{sm}^{Cl} with imposed transmural voltages is described instead by Eq. (8). The curved line, which is a theoretical best fit of the data to the coordinates in Fig. 3, was generated as follows:

1) We assumed that J_c^{NaCl} would not vary with clamping voltage and would be slightly lower than the value shown in Fig. 11 since the mean *Isc* for this group of tissues was lower than the value in Table 1, i.e., $J_c^{NaCl} = 6.4 \times 3.0/3.4 = 5.7$. We also assumed that, while the absolute values of P_j^i might differ from those in Fig. 11, the relations among them would not, i.e., if P_m^{Cl} were 10% lower, each of the other permeabilities would also be 10% lower.

2) Values for μ_m and μ_s were calculated for the 3 imposed voltages (-15, 0, and 10 mV). This was done with Eqs. (2) and (10) for Na and Cl

and the condition $\mu_{ms}=\mu_m-\mu_s$. The permeabilities employed for this initial calculation were those from Fig. 11.

3) P_m^{Cl} was then estimated by the method of least squares as the slope of the following rearrangement of Eq. (8):

$$J_{sm}^{Cl}=P_m^{Cl}[C_0 V_m^{Cl} R_s^{Cl} V_s^{Cl} e^{\mu_s}/(V_m^{Cl}+R_s^{Cl} V_s^{Cl})]+Y_0$$

where Y_0 is the Y-intercept and $R_s^{Cl}=P_s^{Cl}/P_m^{Cl}$, using the permeabilities in Fig. 11.

4) With the new value for P_m^{Cl} (and the corresponding values for the other permeabilities), we next repeated steps *2* and *3* until P_m^{Cl} became constant. Only one repetition proved necessary.

5) Step *2* was now repeated for a wide variety of transmural voltages. The calculated values of μ_m and μ_s were then substituted into Eq. (8) to generate values for J_{sm}^{Cl}.

References

1. Ando, M. 1975. Intestinal water transport and chloride pump in relation to sea-water adaptation of the eel, *Anguilla japonica*. *Comp. Biochem. Physiol.* **52A**:229
2. Ando, M., Utida, S., Nagahama, H. 1975. Active transport of chloride in eel intestine with special reference to sea water adaptation. *Comp. Biochem. Physiol.* **51A**:27
3. Armstrong, W.McD. 1976. Bioelectric parameters and sodium transport in bullfrog small intestine. *In:* Intestinal Ion Transport. J.W.L. Robinson, editor. MTP Press, Lancaster
4. Barry, P.H., Diamond, J.M., Wright, E.M. 1971. The mechanism of cation permeation in rabbit gallbladder: Dilution potentials and biionic potentials. *J. Membrane Biol.* **4**:358
5. Bindslev, N., Tormey, J.M., Wright, E.M. 1974. The effects of electrical and osmotic gradients on lateral intercellular spaces and membrane conductance in a low resistance epithelium. *J. Membrane Biol.* **19**:357
6. Burg, M.B., Green, N. 1973. Function of the thick ascending limb of Henle's loop. *Am. J. Physiol.* **224**:659
7. Cardell, R.R., Jr., Badenhausen, S., Porter, K.R. 1967. Intestinal triglyceride absorption in the rat. An electron microscopical study. *J. Cell Biol.* **34**:123
8. Curry, E. 1939. The histology of the digestive tube of the carp *(Cyprinus carpio communis)*. J. Morphol. **65**:53
9. Dawes, B. 1929. The histology of the alimentary tract of the plaice *(Pleuronectes platessa)*. *Q. J. Microsc. Sci.* **73**:243
10. Desjeux, J.F., Tai, Y.H., Curran, P.F. 1974. Characteristics of sodium flux from serosa to mucosa in rabbit ileum. *J. Gen. Physiol.* **64**:274
11. Diamond, J.M. 1962. The mechanism of solute transport by the gall bladder. *J. Physiol. (London)* **161**:474
12. Field, M., Fromm, D., McColl, I. 1971. Ion transport in rabbit ileal mucosa. I. Na and Cl fluxes and short-circuit current. *Am. J. Physiol.* **220**:1388
13. Frizzell, R.A., Dugas, M.C., Schultz, S.G. 1975. Sodium chloride transport by rabbit gallbladder. Direct evidence for a coupled NaCl influx process. *J. Gen. Physiol.* **65**:769

14. Frizzell, R.A., Nellans, H.N., Rose, R.C., Schultz, S.G. 1973. Intracellular Cl concentrations and influxes across the brush border of rabbit ileum. *Am. J. Physiol.* **224**:328
15. Frömter, E. 1972. The route of passive ion movement through the epithelium of *Necturus* gallbladder. *J. Membrane Biol.* **8**:259
16. Gauthier, G.F., Landis, S.C. 1972. The relationship of ultrastructural and cytochemical features to absorptive activity in the goldfish intestine. *Anat. Rec.* **172**:675
17. Gilles-Baillien, M., Schoffeniels, E. 1967. Fluxes of inorganic ions across the isolated intestinal epithelium of the Greek tortoise. *Arch. Int. Physiol. Biochim.* **75**:754
18. Goldman, D.E. 1943. Potential, impedence and rectification in membranes. *J. Gen. Physiol.* **27**:37
19. Gomori, G. 1955. Preparation of buffers for use in enzyme studies. *In:* Methods in Enzymology. S.P. Colowich and N.O. Kaplan, editors. Vol. 1, p. 138. Academic Press., New York
20. Hendrix, T.R., Bayless, T.M. 1970. Digestion: Intestinal secretion. *Annu. Rev. Physiol.* **32**:139
21. Hirano, T., Morisawa, M., Ando, M., Utida, S. 1976. Adaptive changes in ion and water transport mechanisms in the eel intestine. *In:* Intestinal Ion Transport, p. 301. J.W.L. Robinson, editor. MTP Press, Lancaster
22. House, C.R., Green, K. 1965. Ion and water transport in isolated intestine of the marine teleost, *Cottus scorpius*. *J. Exp. Biol.* **42**:177
23. Huang, K.C., Chen, T.S.T. 1971. Ion transport across intestinal mucosa of winter flounder, *Pseudopleuronectes americanus*. *Am. J. Physiol.* **220**:1734
24. Iwai, T. 1968. Fine structure and absorption patterns of intestinal epithelial cells in rainbow trout *alevins*. *Z. Zellforsch.* **91**:366
25. Kaye, G.I., Wheeler, H.O., Whitlock, R.T., Lane, N. 1966. Fluid transport in the rabbit gall bladder. A combined physiological and electron microscopic study. *J. Cell Biol.* **30**:237
26. Luft, J.H. 1961. Improvements in epoxy resin embedding methods. *J. Biophys. Biochem. Cytol.* **9**:409
27. Machen, T.E., Diamond, J.M. 1969. An estimate of the salt concentration in the lateral intercellular spaces of rabbit gall-bladder during maximal fluid transport. *J. Membrane Biol.* **1**:194
28. Martin, B.J., Philpott, C.W. 1973. The adaptive response of the salt glands of adult mallard ducks to a salt water regime: An ultrastructural and tracer study. *J. Exp. Zool.* **186**:111
29. Martin, D.W. 1974. The effect of the bicarbonate ion on the gallbladder salt pump. *J. Membrane Biol.* **18**:219
30. Martin, D.W., Diamond, J.M. 1966. Energetics of coupled active transport of sodium and chloride. *J. Gen. Physiol.* **50**:295
31. Maunsbach, A.B. 1966. The influence of different fixatives and fixation methods on the ultrastructure of rat kidney proximal tubule cells. I. Comparison of different perfusion fixation methods and of glutaraldehyde, formaldehyde and osmium tetroxide fixatives. *J. Ultrastruct. Res.* **15**:242
32. Millonig, G. 1961. Advantages of a phosphate buffer for OsO_4 solutions in fixation. *J. Appl. Phys.* **32**:1637*A*
33. Nellans, H.N., Frizzell, R.A., Schultz, S.G. 1973. Coupled sodium-chloride influxes across the brush border of rabbit ileum. *Am. J. Physiol.* **225**:467
34. Nellans, H.N., Frizzell, R.A., Schultz, S.G. 1974. Brush-border processes and transepithelial Na and Cl transport by rabbit ileum. *Am. J. Physiol.* **226**:1131
35. Oide, M. 1973. Role of alkaline phosphatase in intestinal water absorption by eels adapted to sea water. *Comp. Biochem. Physiol.* **46A**:639

36. Quay, J.F., Armstrong, W.M. 1969. Sodium and chloride transport by isolated bullfrog small intestine. *Am. J. Physiol.* **217**:694
37. Revel, J.P., Karnovsky, M.J. 1967. Hexagonal array of subunits in intercellular junctions of the mouse heart and liver. *J. Cell Biol.* **33**:C7
38. Reynolds, E.S. 1963. The use of lead citrate at high pH as an electron opaque stain in electron microscopy. *J. Cell Biol.* **17**:208
39. Richardson, K.C., Jarrett, L., Finke, E.H. 1960. Embedding in epoxy resins for ultrathin sectioning in electron microscopy. *Stain Technol.* **35**:313
40. Ritch, R., Philpott, C.W. 1969. Repeating particles associated with an electrolyte-transport membrane. *Exp. Cell Res.* **55**:17
41. Schultz, S.G., Frizzell, R.A. 1976. Ionic permeability of epithelial tissues. *Biochim. Biophys. Acta* **443**:181
42. Sheerin, H.E., Field, M. 1975. Ileal HCO_3 secretion: Relationship to Na and Cl transport and effect of theophylline. *Am. J. Physiol.* **228**:1065
43. Smith, M.W., Ellory, J.C., Lahlou, B. 1975. Sodium and chloride transport by the intestine of the European flounder *Platichthys flesus* adapted to fresh or sea water. *Pfluegers Arch.* **357**:303–312
44. Tasso, F. 1974. Diversite d'aspect tes fibres neurosécrétrices révélées dans la post-hypophyse du Rat par la technique de postfixation combinant l'osmium et le ferrocyanure de potassium. *C.R. Seances Soc. Biol. Fil.* **168**:986
45. Toner, P.G. 1968. Cytology of intestinal epithelial cells. *Int. Rev. Cytol.* **24**:233
46. Tormey, J.M., Diamond, J.M. 1967. The ultrastructural route of fluid transport in rabbit gall bladder. *J. Gen. Physiol.* **50**:2031
47. Trier, J.S. 1968. Morphology of the epithelium of the small intestine. *In:* Handbook of Physiology. Section 6: Alimentary Canal. Vol. III, p. 1125. C.F. Code, editor. American Physiological Society, Washington, D.C.
48. Van Lennep, E.W. 1968. Electron microscopic histochemical studies on salt-excreting glands in elasmobranch and marine catfish. *J. Ultrastruct. Res.* **25**:94
49. Yamamoto, T. 1966. An electron microscope study of the columnar epithelial cell in the intestine of fresh water teleosts: Goldfish *(Carassius auratus)* and rainbow trout *(Salmo irideus)*. *Z. Zellforsch.* **72**:66